

# **Circuit Quantum Electrodynamics**

## **Superconducting platform**

### **(11th Lecture)**

Covering: basic concepts, measurement techniques,  
implementations, qubit approaches, current trends

With figures and slides borrowed from

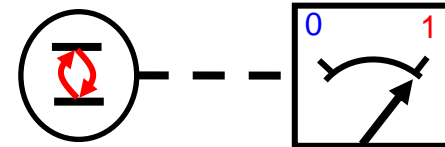
P. Bertet (CEA Saclay), C. Eichler (FAU Erlangen), L. Di Carlo (TU Delft)

# Requirements for QC

**High-Fidelity  
Single Qubit Operations**



**High-Fidelity Readout  
of Individual Qubits**



**Deterministic, On-Demand  
Entanglement between Qubits**



Two-qubit operations  
mediated by a resonator  
(quantum bus)

# Examples of static qubit-qubit couplers

Direct capacitive coupling:

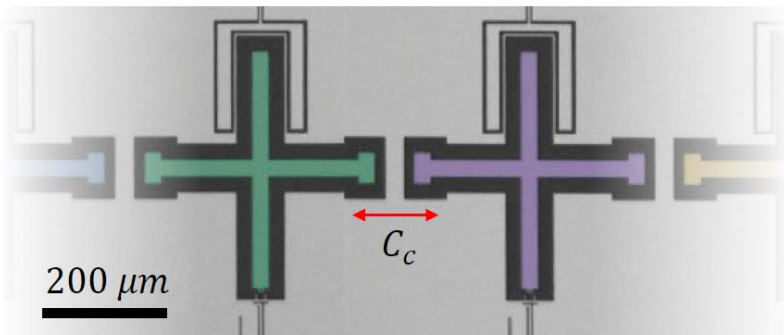


Image: Barends et al., Nature (2016)

Properties:

- Coupling strength  $J = \frac{c_c}{2\sqrt{c_1 c_2}} \sqrt{\omega_1 \omega_2}$  can be made large.
- Qubits are in near vicinity of each other.
- No need for an additional coupling element introducing an extra mode.

Coupling mediated by a resonator

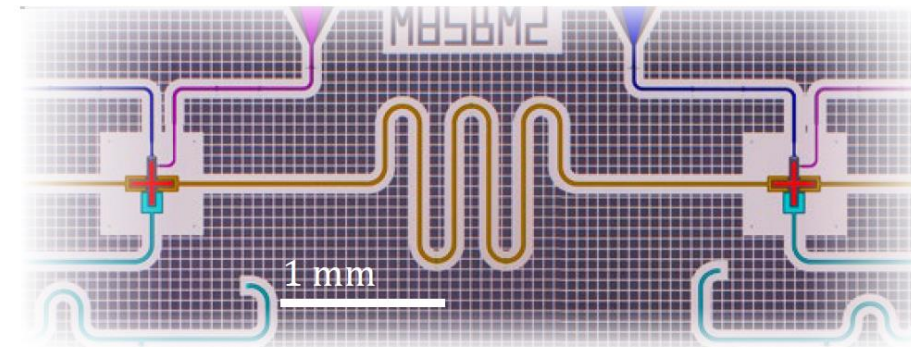


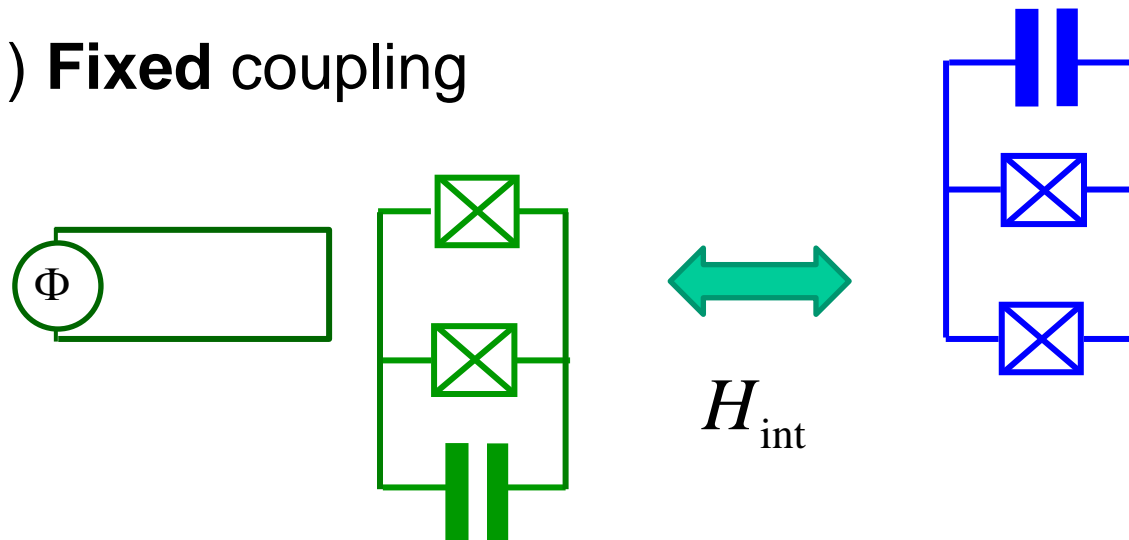
Image: Heinsoo et al., PR Applied (2018)

Properties:

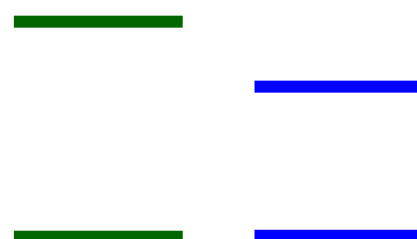
- Coupling strength depends on the detuning between qubits and resonator.
- Multiple qubits can be coupled to a common resonator acting as a BUS
- Coupling mediated over “long” distance on the chip. Qubits can be spatially separated on the chip.

# Coupling strategies

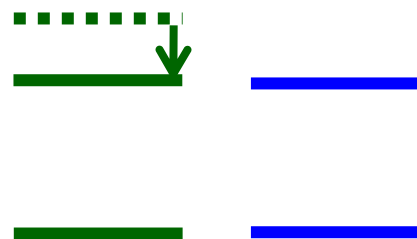
## 1) Fixed coupling



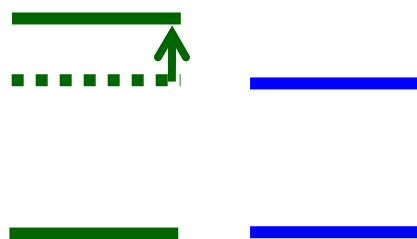
Entanglement on-demand ???  
« Tune-and-go » strategy



Coupling  
**effectively** OFF



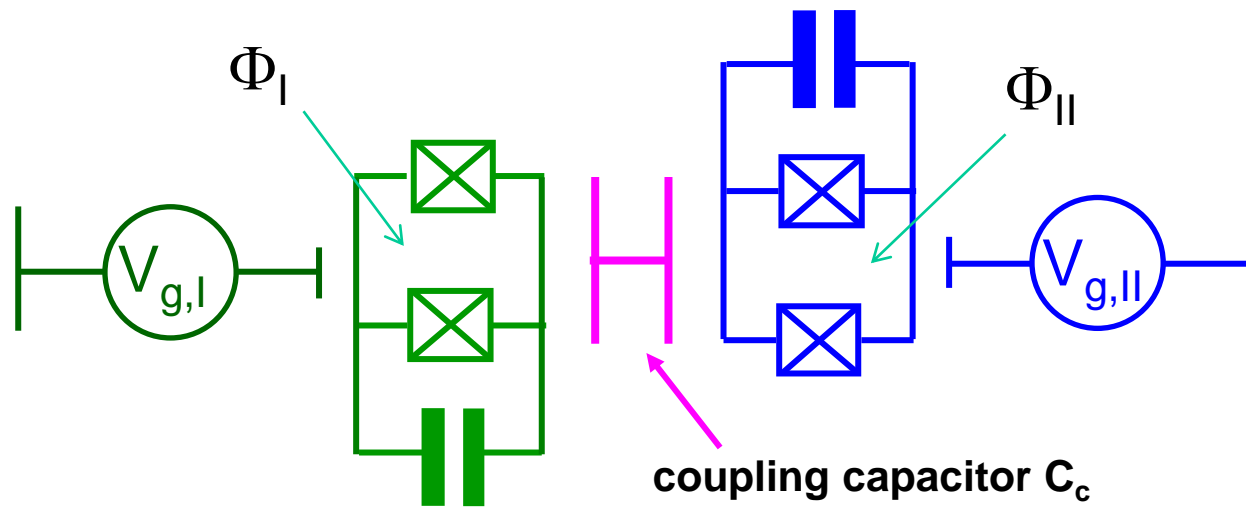
Coupling activated  
in resonance for  $\tau$



**Entangled** qubits  
Interaction effectively OFF

# Coupling strategies

## 1) Direct capacitive coupling



$$\begin{aligned}
 H = & E_{c,I}(\hat{N}_I - N_{g,I}) - E_{J,I}(\Phi_I) \cos \hat{\theta}_I \\
 & + E_{c,II}(\hat{N}_{II} - N_{g,II}) - E_{J,II}(\Phi_{II}) \cos \hat{\theta}_{II} \\
 & + 2 \frac{E_{c,I} E_{c,II}}{E_{cc}} (\hat{N}_I - N_{g,I})(\hat{N}_{II} - N_{g,II})
 \end{aligned}$$

$$\hbar g = (2e)^2 \frac{C_c}{C_I C_{II}} \left| \langle 0_I | \hat{N}_I | 1_I \rangle \langle 0_{II} | \hat{N}_{II} | 1_{II} \rangle \right|$$

$$\begin{cases}
 H_{q,I} = -\frac{\hbar \omega_{01}^I(\Phi_I)}{2} \sigma_{z,I} \\
 H_{q,II} = -\frac{\hbar \omega_{01}^{II}(\Phi_{II})}{2} \sigma_{z,II} \\
 H_c = \hbar g \sigma_{x,I} \sigma_{x,II} \\
 \sim \hbar g (\sigma_I^+ \sigma_{II}^- + \sigma_I^- \sigma_{II}^+)
 \end{cases}$$

courtesy CEA Saclay

# iSWAP Gate

$$H / \hbar = -\frac{\omega_{01}^I}{2} \sigma_z^I - \frac{\omega_{01}^{II}}{2} \sigma_z^{II} + g \left( \sigma_+^I \sigma_-^{II} + \sigma_-^I \sigma_+^{II} \right)$$

$H_{\text{int}}$

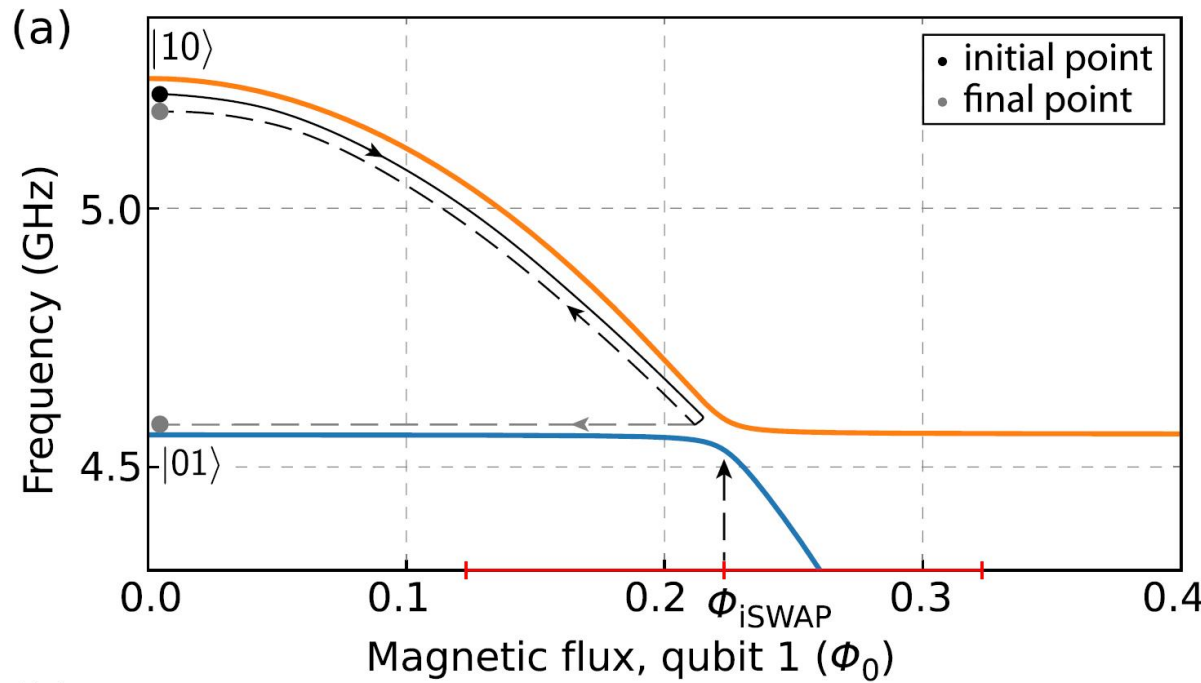
→ « Natural » universal gate :  $\sqrt{i\text{SWAP}}$

On resonance, ( $\omega_{01}^I = \omega_{01}^{II}$ )

$$U_{\text{int}}(t) = \begin{bmatrix} \textbf{OO} & \textbf{1O} & \textbf{O1} & \textbf{11} \\ 1 & 0 & 0 & 0 \\ 0 & \cos(gt) & -i \sin(gt) & 0 \\ 0 & -i \sin(gt) & \cos(gt) & 0 \\ 0 & 0 & 0 & 1 \end{bmatrix} \quad U_{\text{int}}\left(\frac{\pi}{2g}\right) = \boxed{\begin{bmatrix} 1 & 0 & 0 & 0 \\ 0 & 1/\sqrt{2} & -i/\sqrt{2} & 0 \\ 0 & -i/\sqrt{2} & 1/\sqrt{2} & 0 \\ 0 & 0 & 0 & 1 \end{bmatrix}} = \sqrt{i\text{SWAP}}$$

# Coupling strategies: direct capacitive coupling

## Experiment



Applied Physics Reviews 6, 021318 (2019)

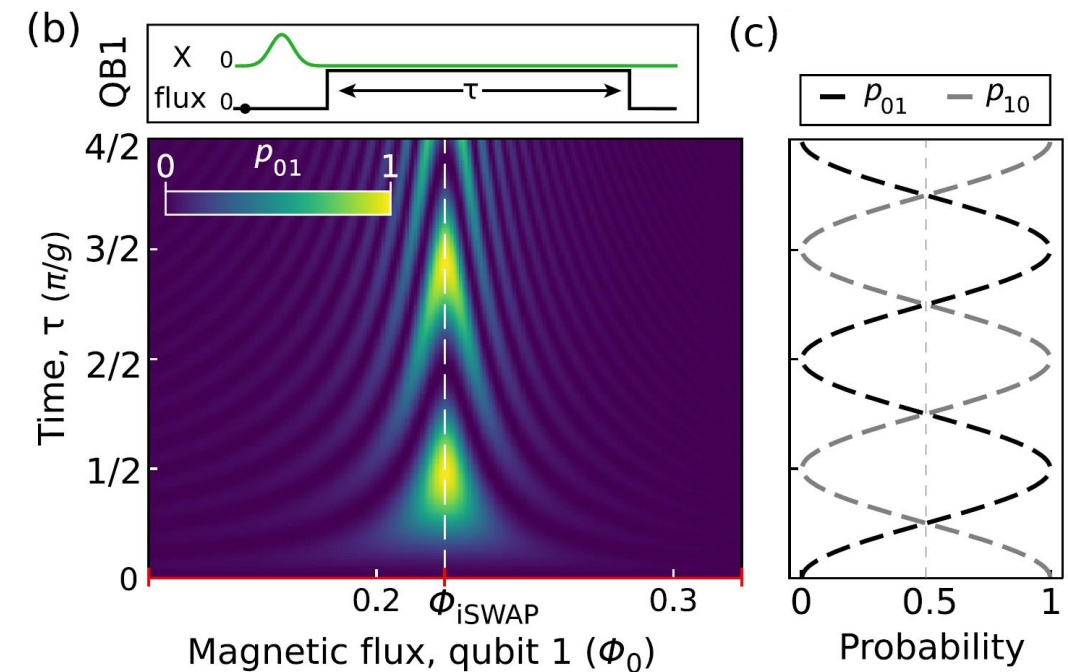
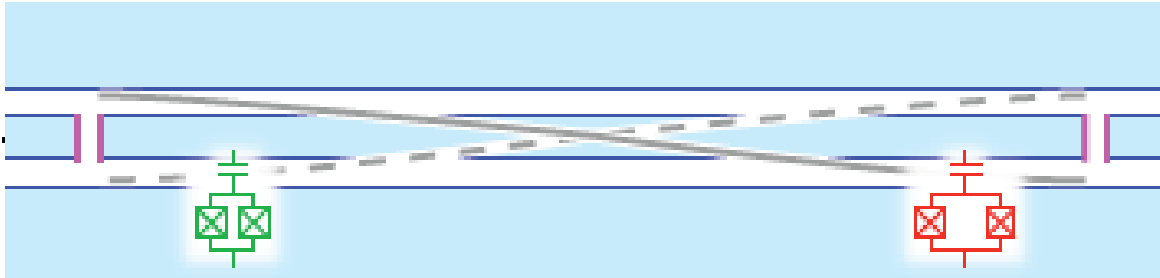
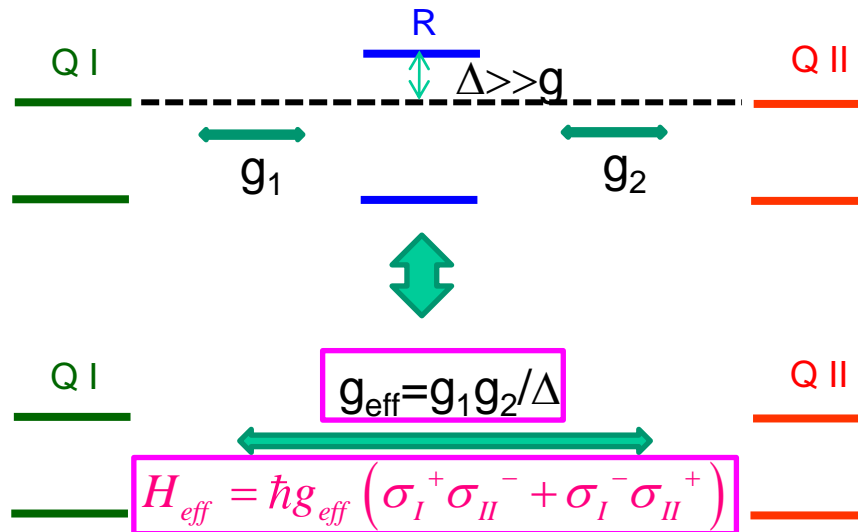


**FIG. 15.** (a) Spectrum of two transmon qubits (written in the combined basis as  $|QB1, QB2\rangle$ ) as the local flux through the loop of qubit 1 is increased. The black/dashed lines with arrows indicate a typical flux trajectory to demonstrate operation of *iSWAP* gate. (b) Probability of swapping into the  $|01\rangle$  state as a function of time and flux. The pulse sequence corresponds to preparing  $|10\rangle$  and performing a typical *iSWAP* operation (for a time  $\tau$ ). (c) Probabilities of  $|01\rangle$  (black) and  $|10\rangle$  (gray) at  $\Phi = \Phi_{iSWAP}$  [white dashed line in (b)] as the time spent at the operating point ( $\tau$ ) is increased. This simulation does not include any decay effects.

# How to couple transmon qubits ? Cavity mediated qubit-qubit coupling



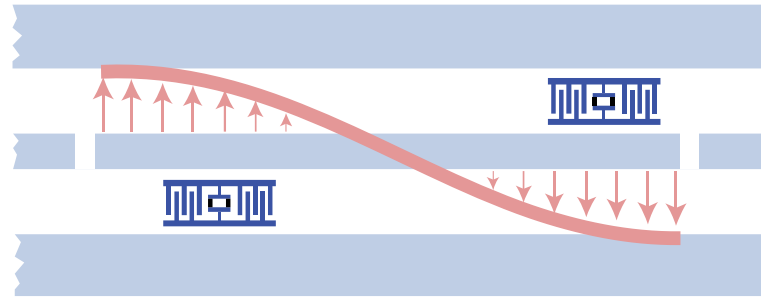
J. Majer et al., Nature 449, 443 (2007)



courtesy CEA Saclay

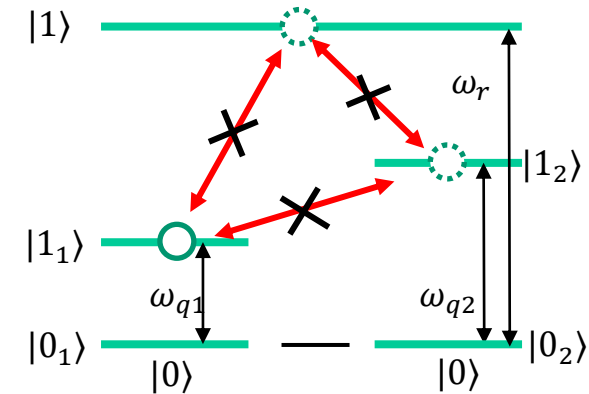
# 2-Qubit gates: using the quantum bus

Two qubits and resonator in dispersive regime  $\Delta_1 = |\omega_{q1} - \omega_r| \sim |\omega_{q1} - \omega_r| \ll g$



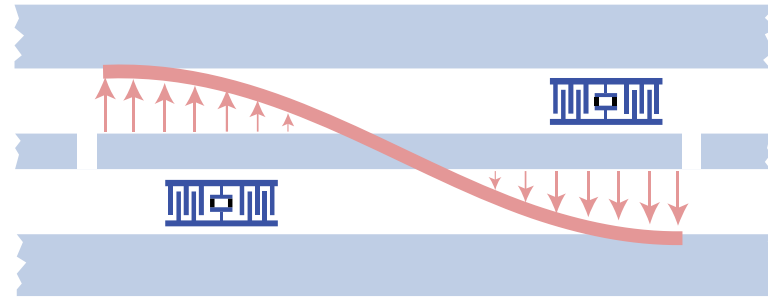
All subsystems are effectively **decoupled**:

- Qubit-resonator transitions are forbidden by **energy conservation**
- No direct qubit-qubit transitions interaction

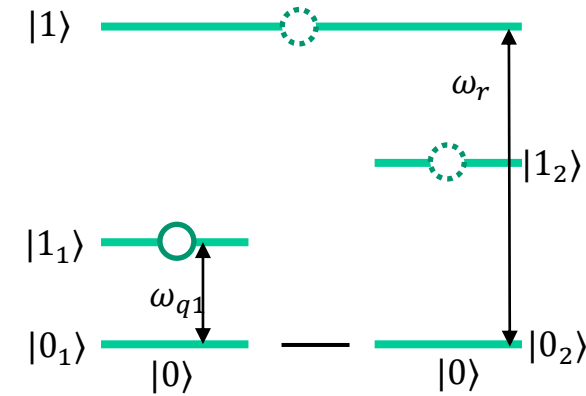


# 2-Qubit gates: using the quantum bus

Two qubits and resonator in dispersive regime  $\Delta_1 = |\omega_{q1} - \omega_r| \sim |\omega_{q1} - \omega_r| \ll g$

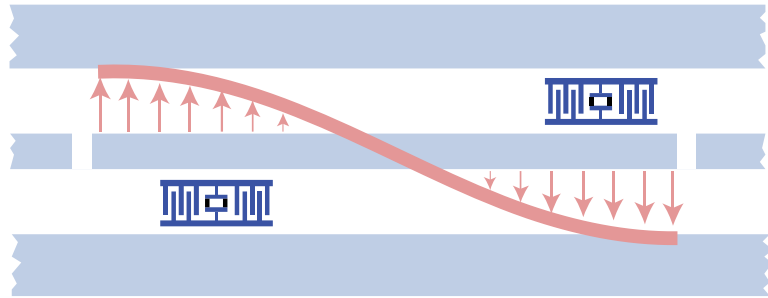


Tune qubits in resonance:



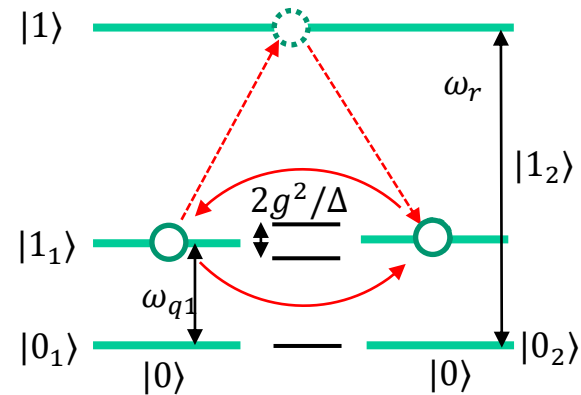
# 2-Qubit gates: using the quantum bus

Two qubits and resonator in dispersive regime  $\Delta_1 = |\omega_{q1} - \omega_r| \sim |\omega_{q1} - \omega_r| \ll g$



Tune qubits in resonance:

- Qubit-qubit interaction **enabled** via virtual photon exchange
- Manifested in **splitting** of  $|0_1 1_2\rangle \leftrightarrow |1_1 0_2\rangle$  (similar to **vacuum Rabi** splitting)
- The splitting is **second order** in  $g/\Delta$

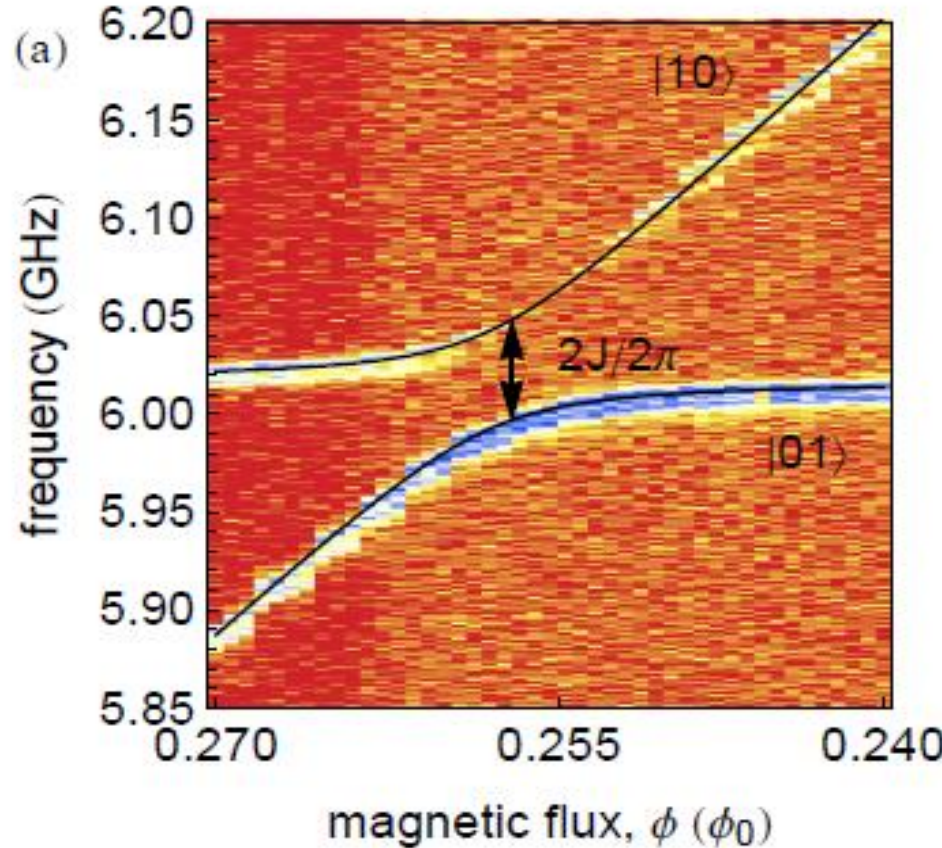


$$H_{int} = J(\sigma^- \sigma^+ + \sigma^+ \sigma^-)$$

**Non-local interaction through photon exchange -> Quantum bus**

# 2-Qubit gates: using the quantum bus

Two qubits and resonator in dispersive regime  $\Delta_1 = |\omega_{q1} - \omega_r| \sim |\omega_{q1} - \omega_r| \ll g$



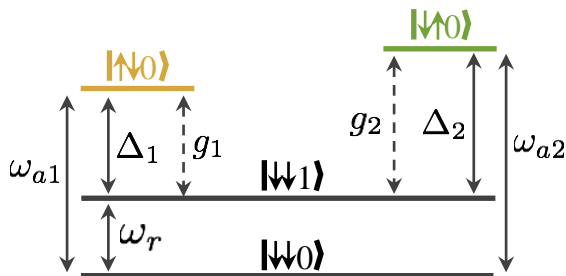
# Coupling via Virtual Photon Exchange

Dispersive two qubit Hamiltonian

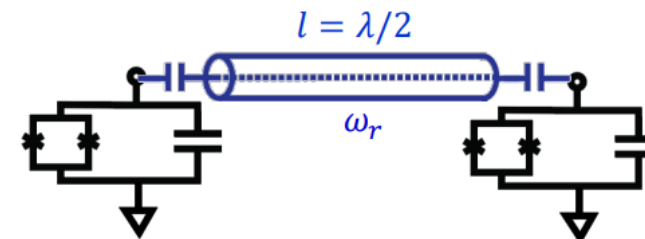
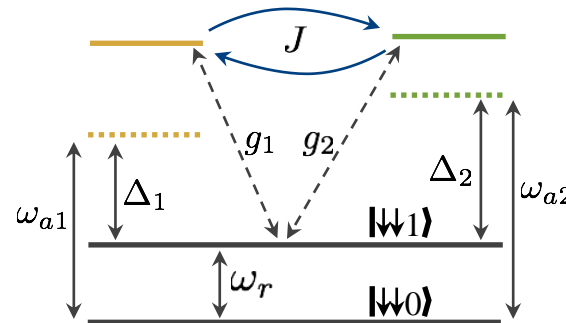
(Tavis-Cummings Hamiltonian):

$$H_{\text{eff}} \approx \omega_r a^\dagger a + \sum_j \frac{1}{2} \left[ \omega_{aj} + 2 \frac{g_j^2}{\Delta_j} \left( a^\dagger a + \frac{1}{2} \right) \right] \sigma_{z_j} + J (\sigma_{-1}\sigma_{+2} + \sigma_{+1}\sigma_{-2})$$

Detuned qubits: interaction suppressed



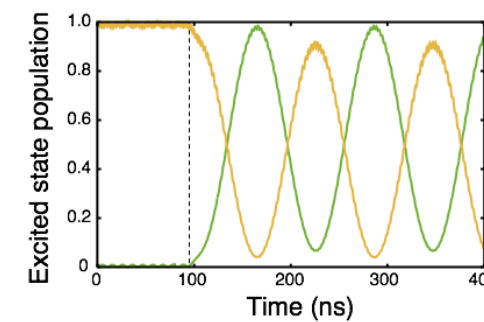
Qubits resonant: virtual photon mediated interaction



Interaction strength:

$$J = \frac{g_1 g_2}{2} \left( \frac{1}{\Delta_1} + \frac{1}{\Delta_2} \right)$$

$\sim 1 - 50$  MHz

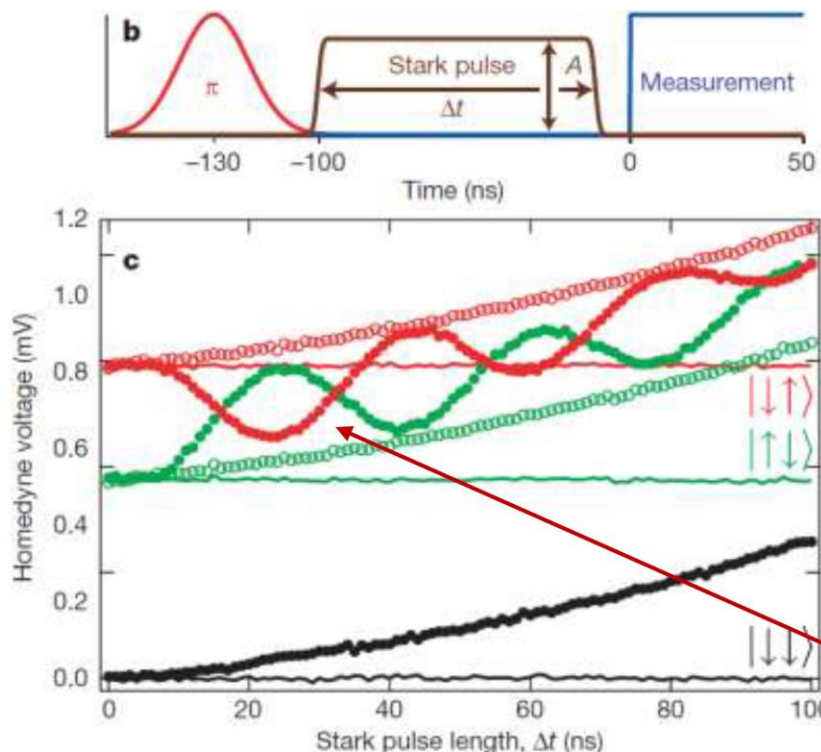


# Dispersive protocol for quantum state transfer

$$\delta_{A,B} \equiv \omega_{A,B} - \omega_r$$

$$\hat{U} = e^{\frac{g}{\delta}(\hat{\sigma}_A^+ \hat{a} - \hat{\sigma}_A^- \hat{a}^\dagger + \hat{\sigma}_B^+ \hat{a} + \hat{\sigma}_B^- \hat{a}^\dagger)}$$

$$\hat{H}^{(2)} = \frac{\hbar\omega_A}{2}\hat{\sigma}_z^A + \frac{\hbar\omega_B}{2}\hat{\sigma}_z^B + \hbar\left(\omega_r + \frac{g^2}{\delta_A}\hat{\sigma}_z^A + \frac{g^2}{\delta_B}\hat{\sigma}_z^B\right)\hat{a}^\dagger\hat{a} + \hbar J(\hat{\sigma}_A^- \hat{\sigma}_B^+ + \hat{\sigma}_A^+ \hat{\sigma}_B^-)$$



## Protocol

- Qubits detuned at different frequencies
  - Coupling off,  $J \simeq 0$
- Bring one qubit to  $|e\rangle$  using a  **$\pi$ -pulse**
- Apply **strong & detuned Stark shift pulse** to bring qubits into resonance
  - $\frac{J}{2\pi} \simeq 23$  MHz for time  $\Delta t$
- After the pulse ( $J \simeq 0$  again) send **readout pulse** to resonator

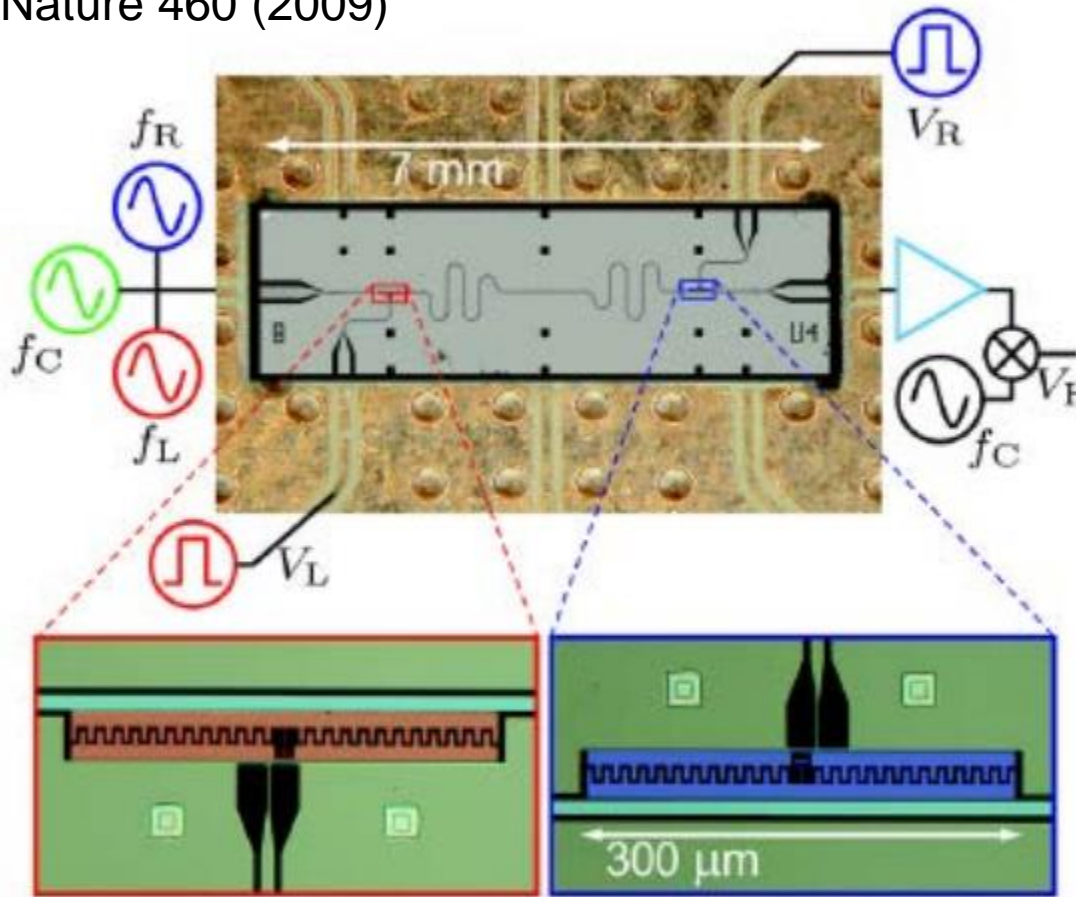
## Results

- Qubits **coherently exchange population**
- Curved slope due to residual Rabi drive by the off-resonant Stark tone

# Control-Phase with two coupled transmons

Applied Physics Reviews 6, 021318 (2019)

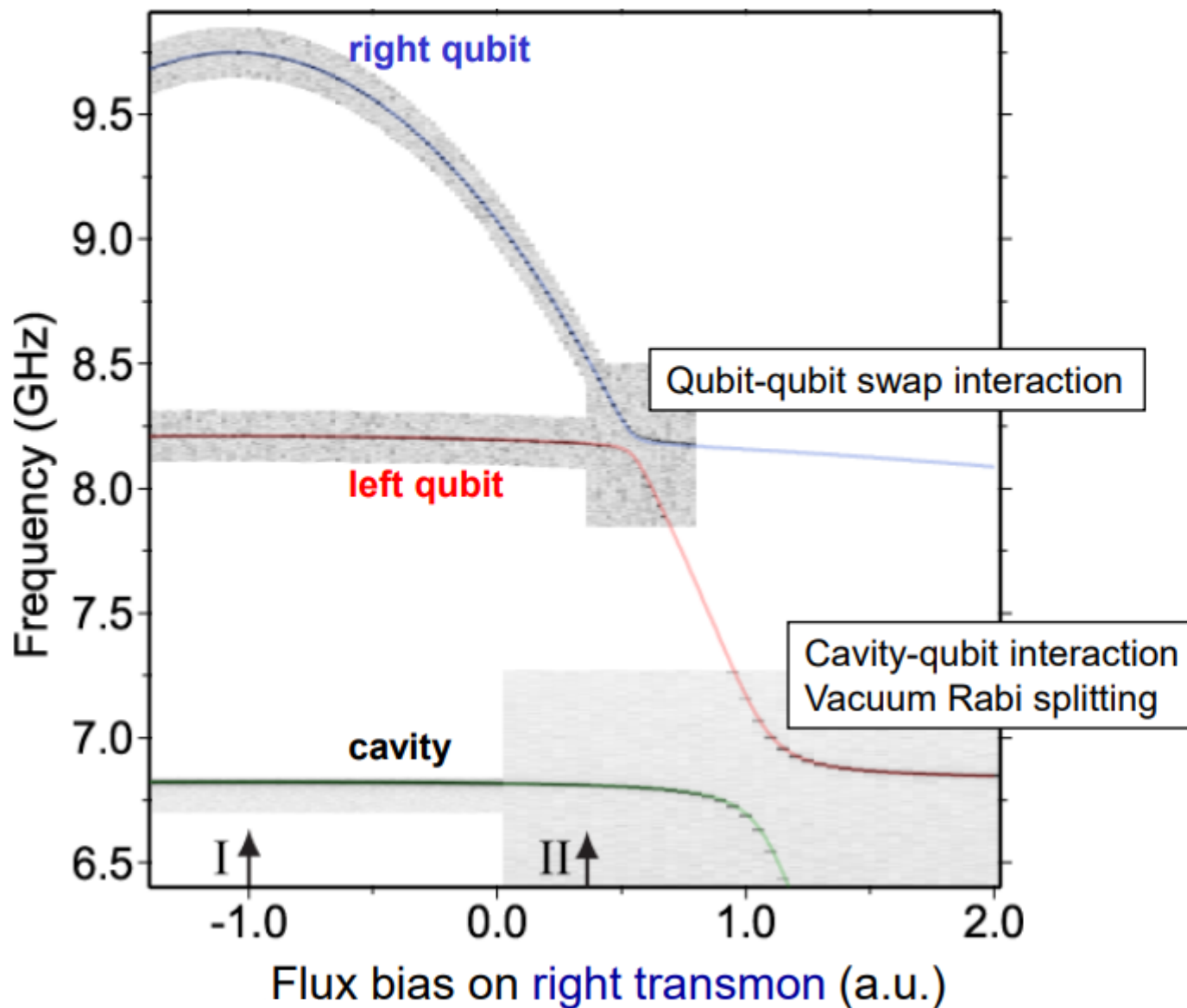
DiCarlo et al., Nature 460 (2009)



$$H_{\text{int}} / \hbar = g_{\text{eff}1} (|1_L 0_R\rangle \langle 0_L 1_R| + h.c) + g_{\text{eff}2} (|1_L 1_R\rangle \langle 0_L 2_R| + h.c)$$

# Spectroscopy of two qubits + cavity

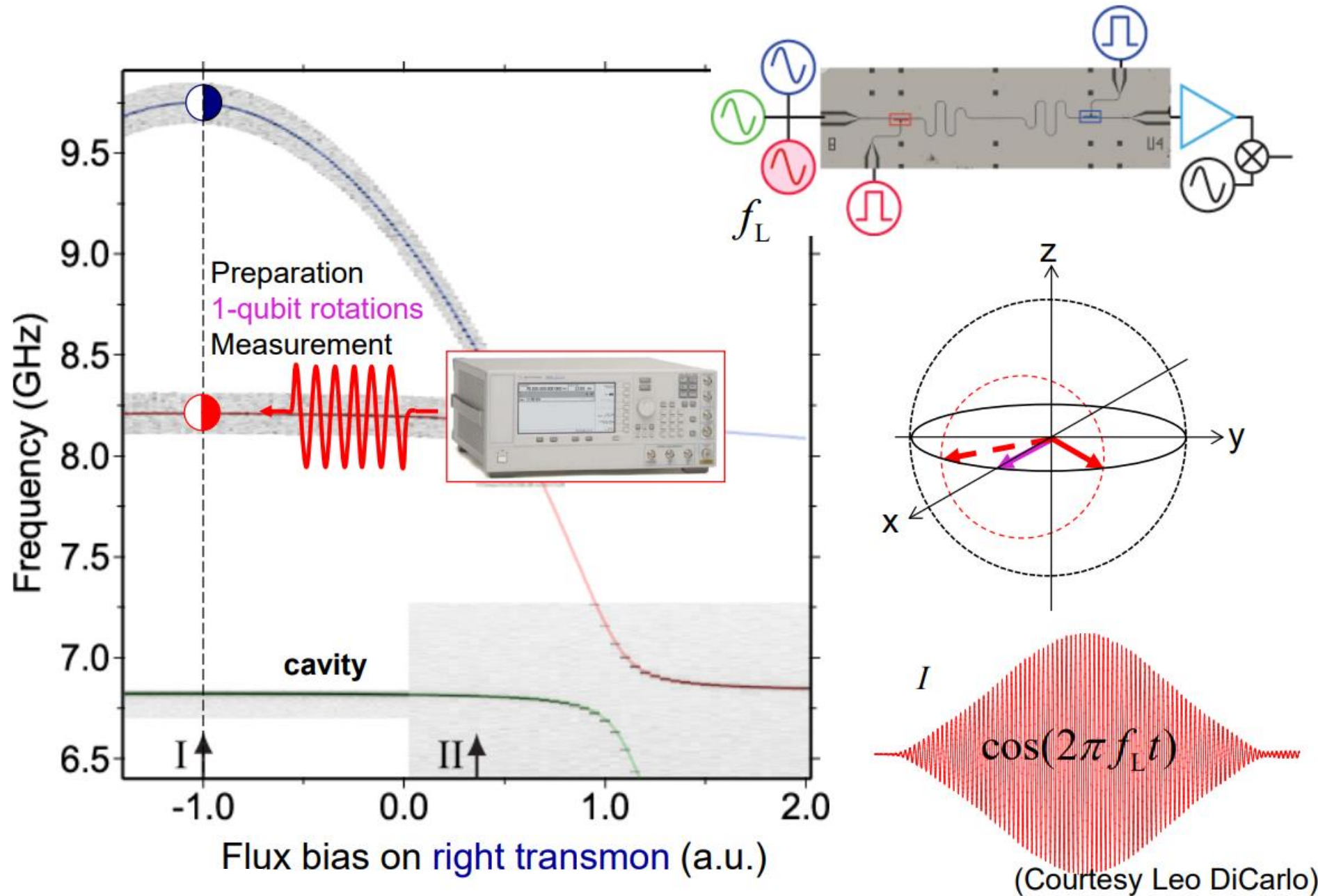
17



(Courtesy Leo DiCarlo)

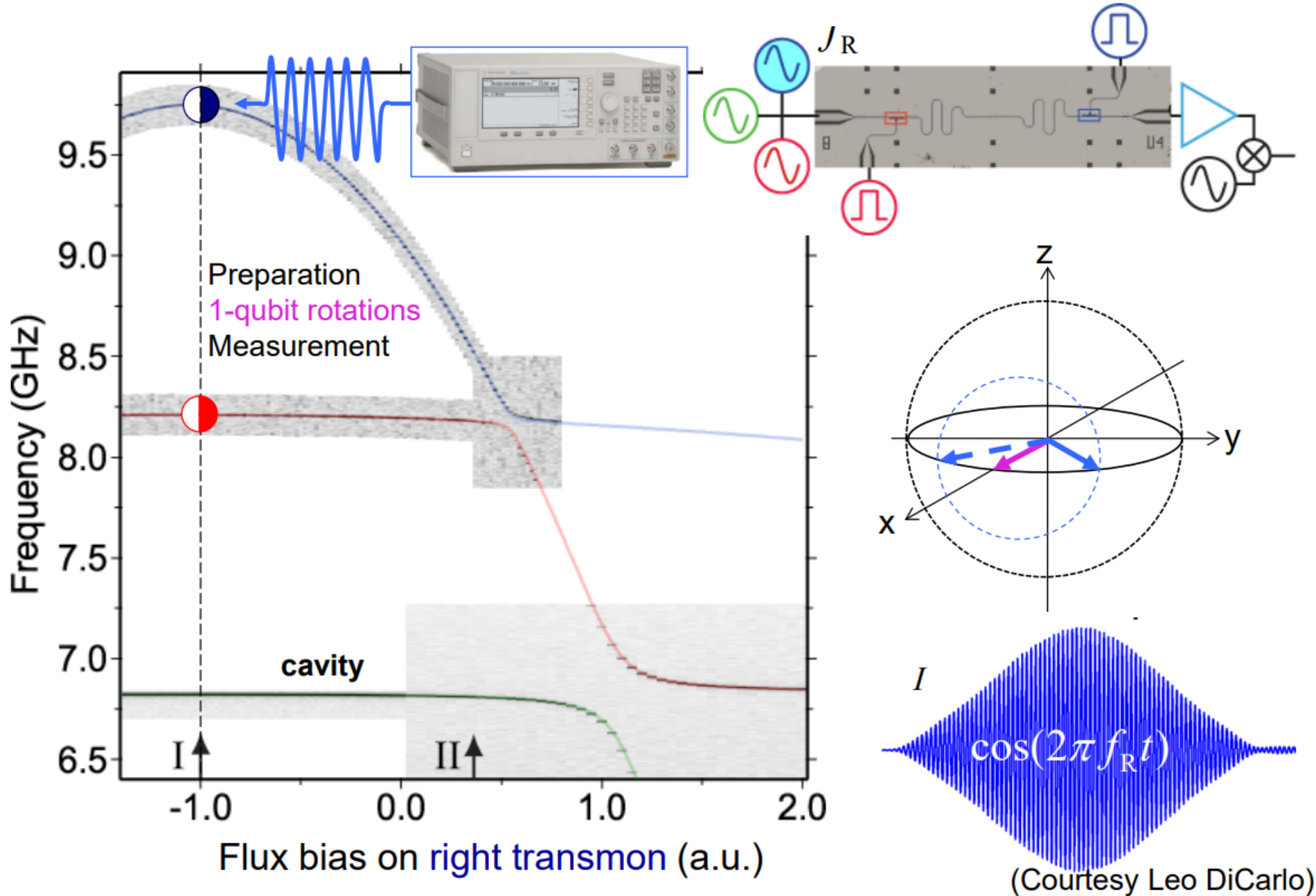
# One-qubit gates: X and Y rotations

18



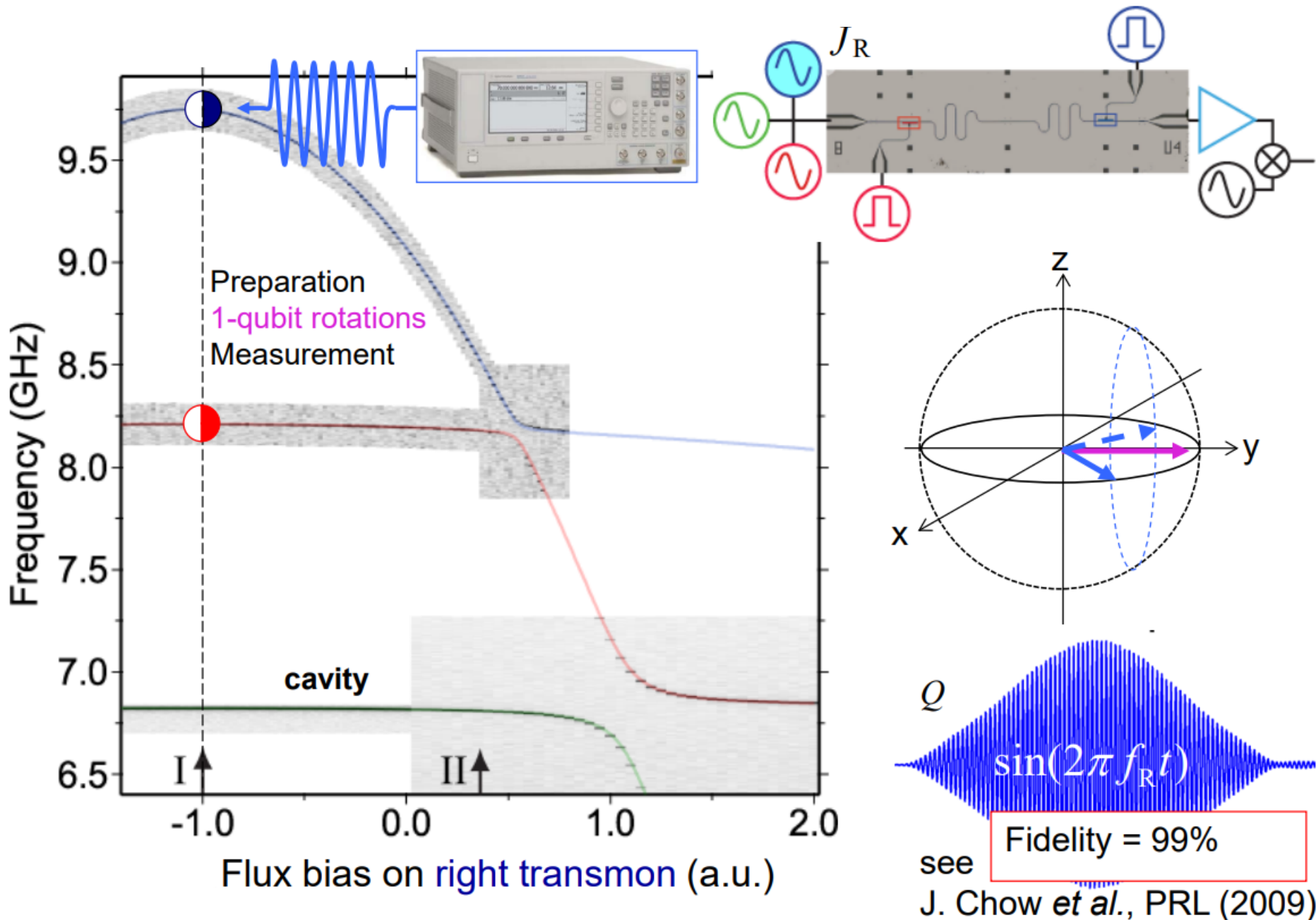
# One-qubit gates: X and Y rotations

19



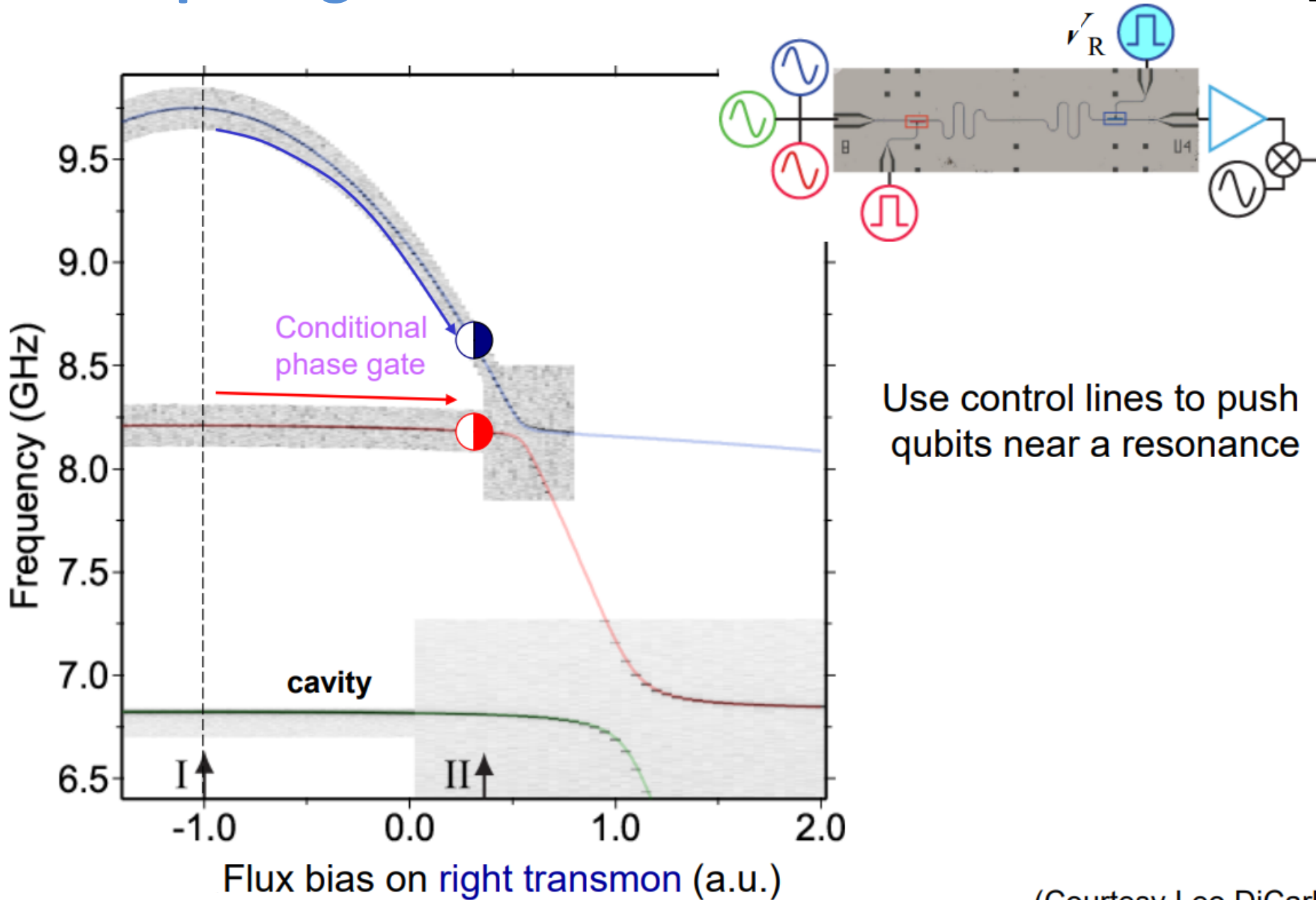
# One-qubit gates: X and Y rotations

20



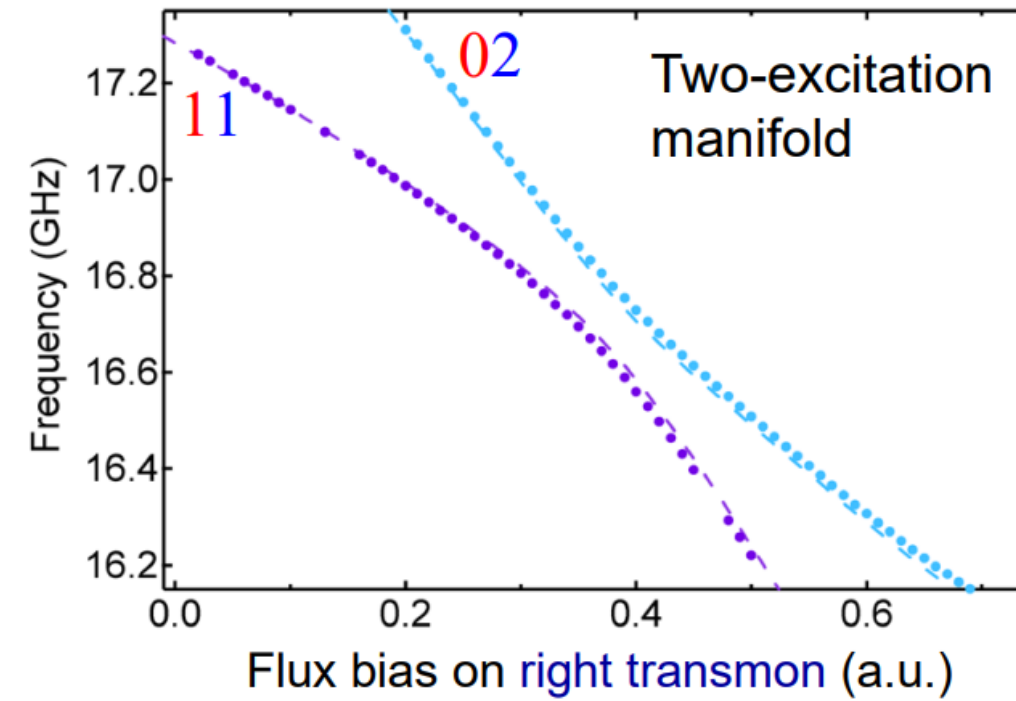
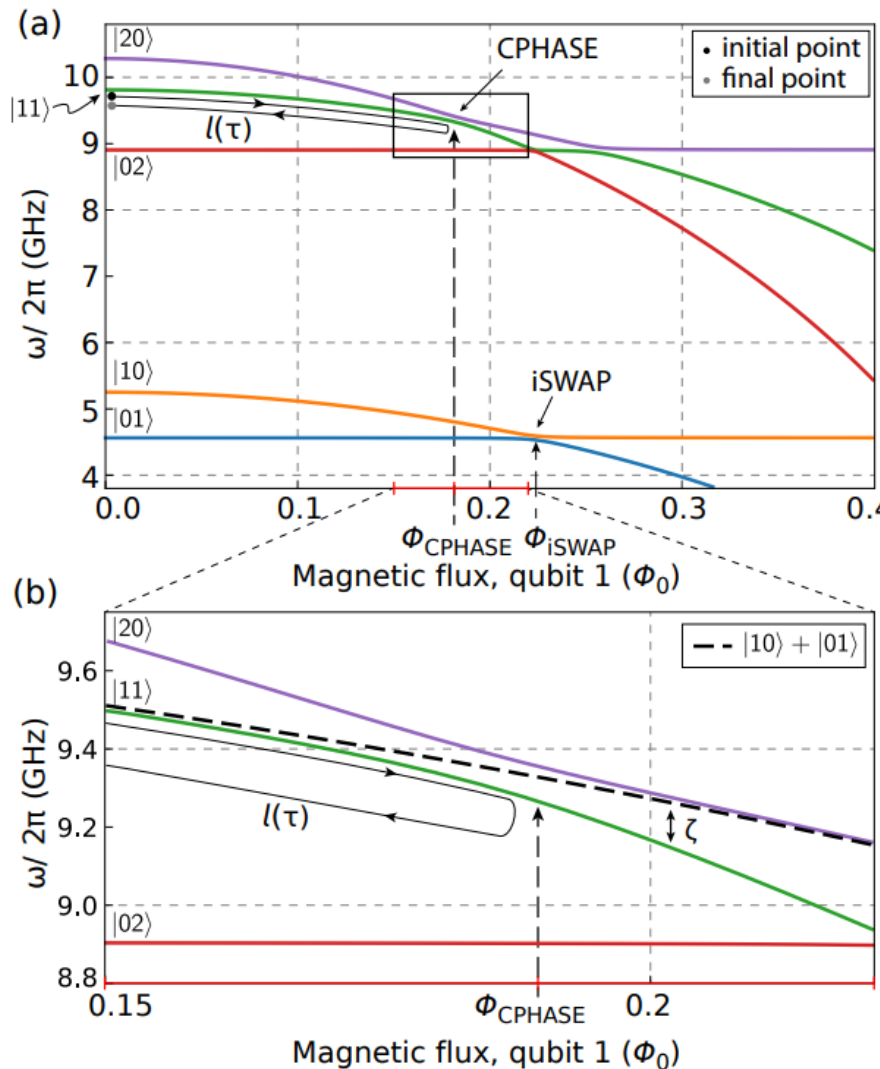
# Two-qubit gate: Turn-On interactions

21



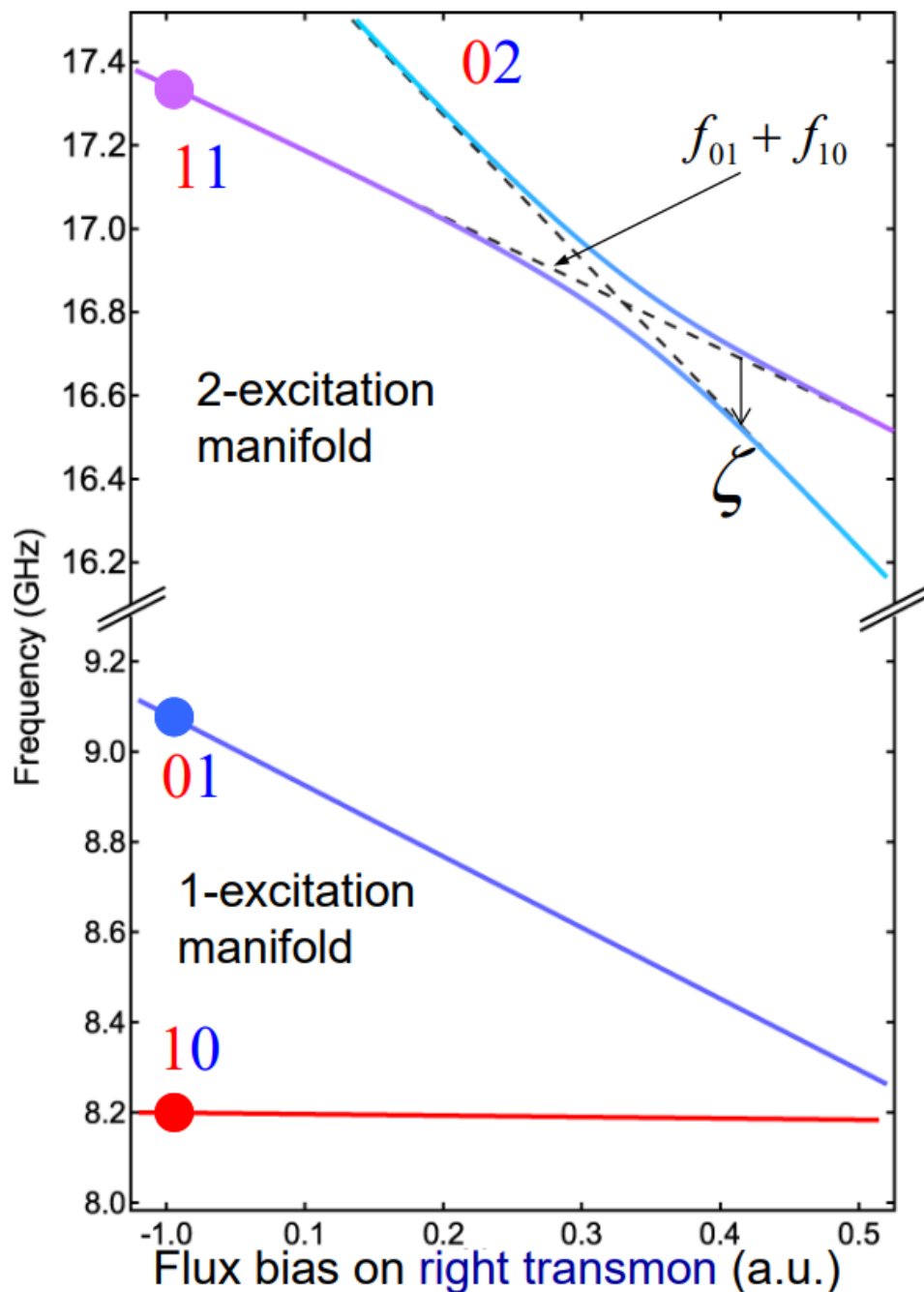
# Two-excitation manifold of the system

22



- Avoided crossing (160 MHz)

$$|11\rangle \leftrightarrow |02\rangle$$



$$\varphi_a = -2\pi \int_{t_0}^{t_f} \delta f_a(t) dt$$

$$|11\rangle \rightarrow e^{i\varphi_{11}} |11\rangle$$

$$\varphi_{11} = \varphi_{10} + \varphi_{01} - 2\pi \int_{t_0}^{t_f} \zeta(t) dt$$

$$|01\rangle \rightarrow e^{i\varphi_{01}} |01\rangle$$

$$|10\rangle \rightarrow e^{i\varphi_{10}} |10\rangle$$

(Courtesy Leo DiCarlo)

# Implementing C-Phase

24

$$U = \begin{pmatrix} |00\rangle & |01\rangle & |10\rangle & |11\rangle \\ 1 & 0 & 0 & 0 \\ 0 & e^{i\phi_{01}} & 0 & 0 \\ 0 & 0 & e^{i\phi_{10}} & 0 \\ 0 & 0 & 0 & e^{i\phi_{11}} \end{pmatrix} |00\rangle \\ |01\rangle \\ |10\rangle \\ |11\rangle$$

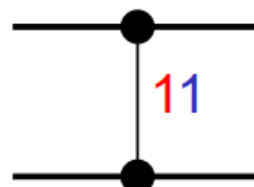
Adjust timing of flux pulse so that only quantum amplitude of  $|11\rangle$  acquires a minus sign:

After the adiabatic excursion, one can now apply single-qubit pulses (or use virtual-Z gates) to exactly cancel the single-qubit phases.

$$|00\rangle |01\rangle |10\rangle |11\rangle$$

$$U = \begin{pmatrix} 1 & 0 & 0 & 0 \\ 0 & 1 & 0 & 0 \\ 0 & 0 & 1 & 0 \\ 0 & 0 & 0 & -1 \end{pmatrix} |00\rangle \\ |01\rangle \\ |10\rangle \\ |11\rangle$$

C-Phase<sub>11</sub>

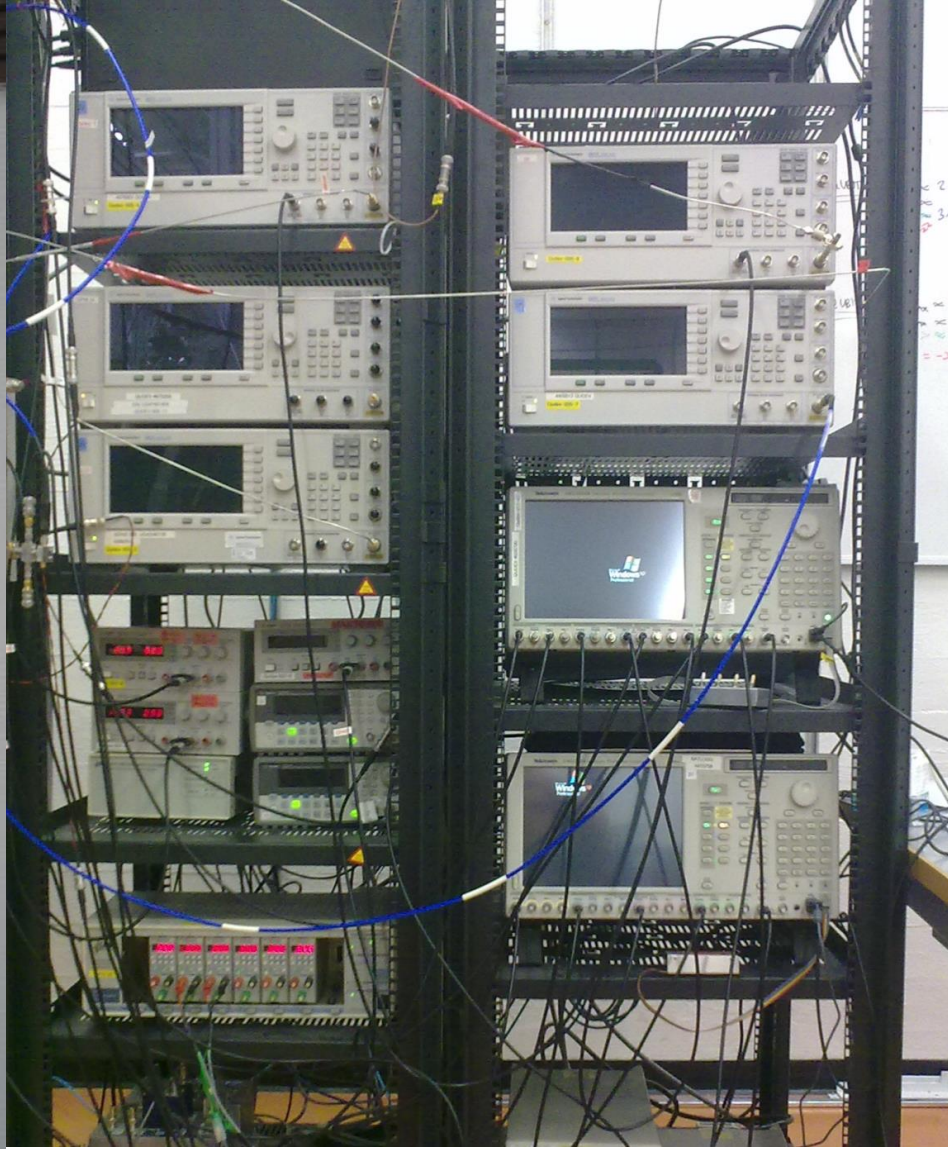


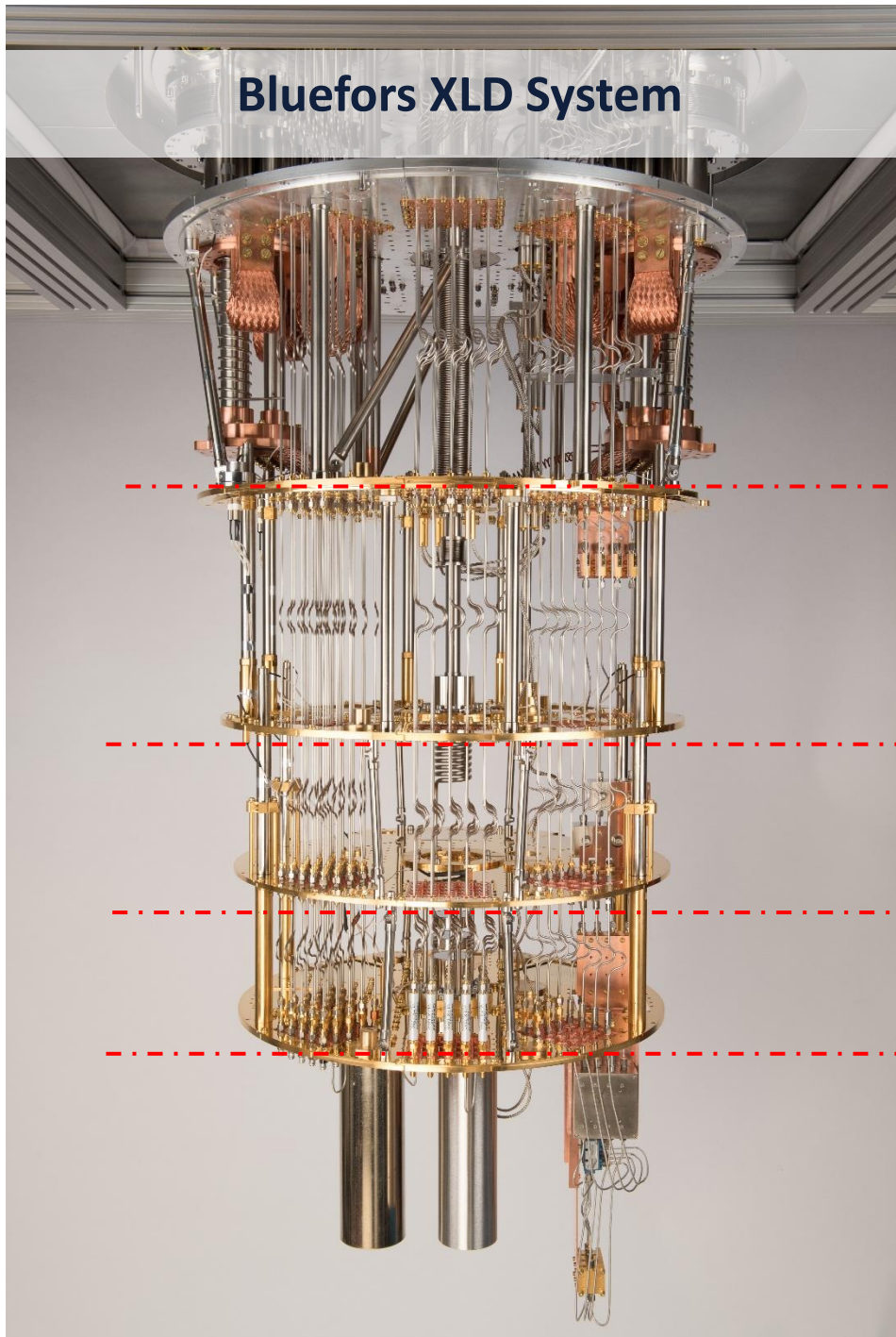
(Courtesy Leo DiCarlo)

# cQED microwave setup



## Microwave Control Electronics





RT

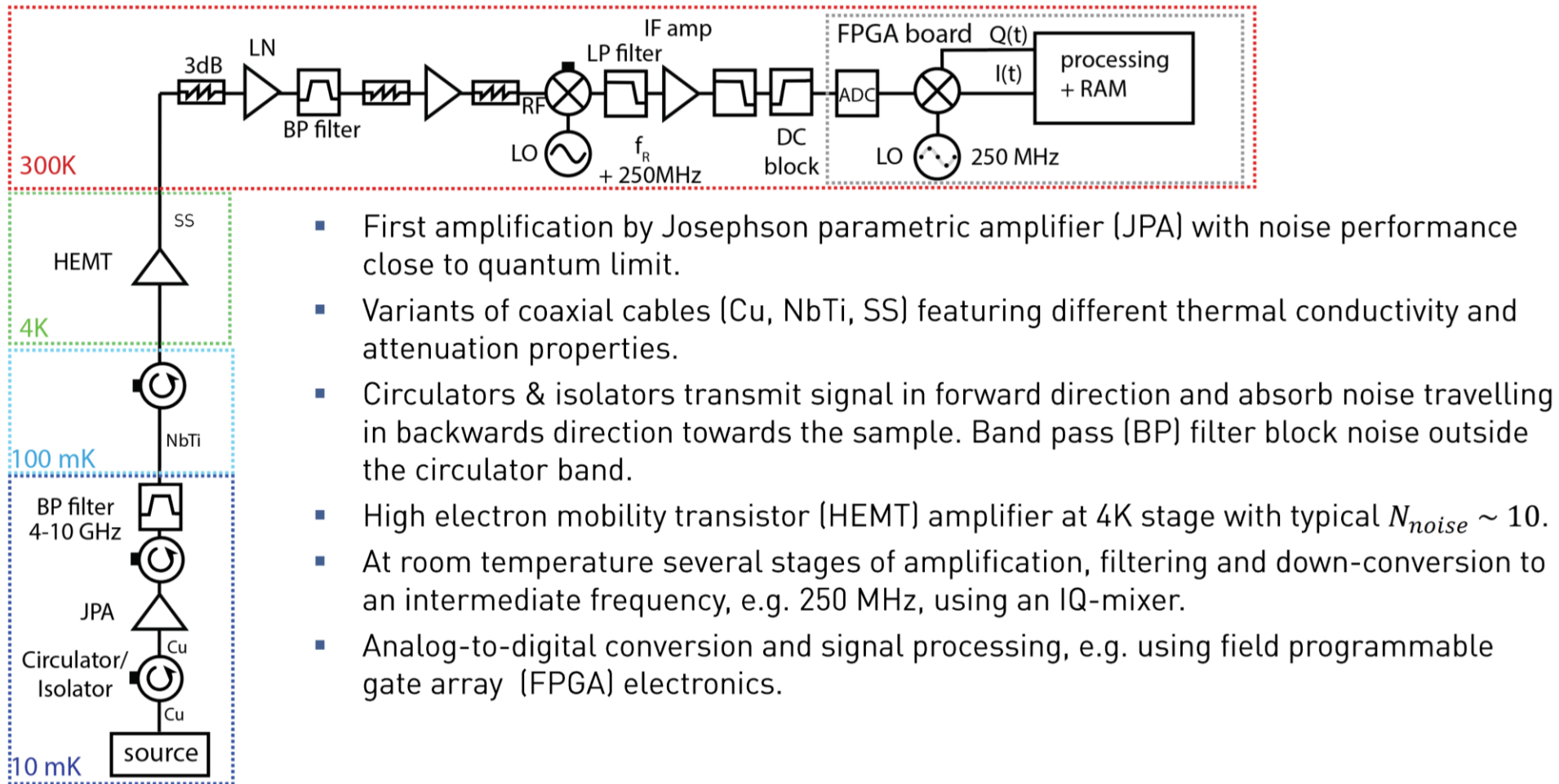
70 K

4 K

800 mK

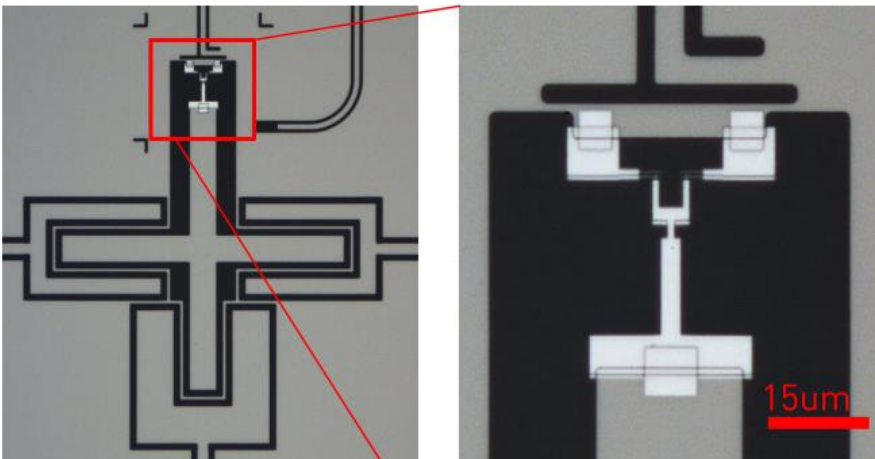
8 mK

# Output Line Configuration: Detection setup



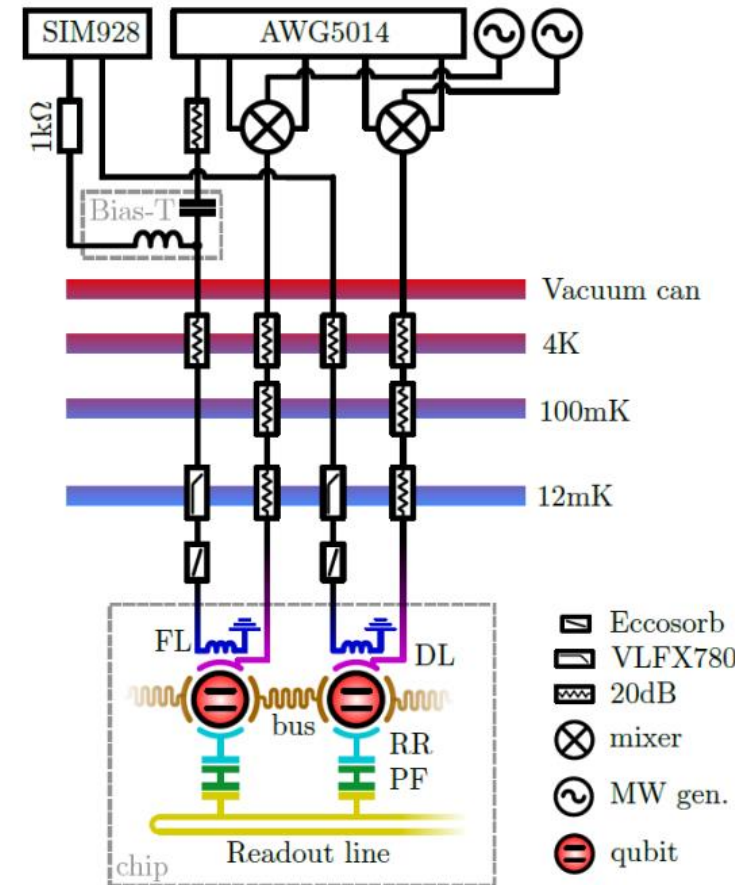
# Qubit Tunability:

## Static (DC) and fast flux control

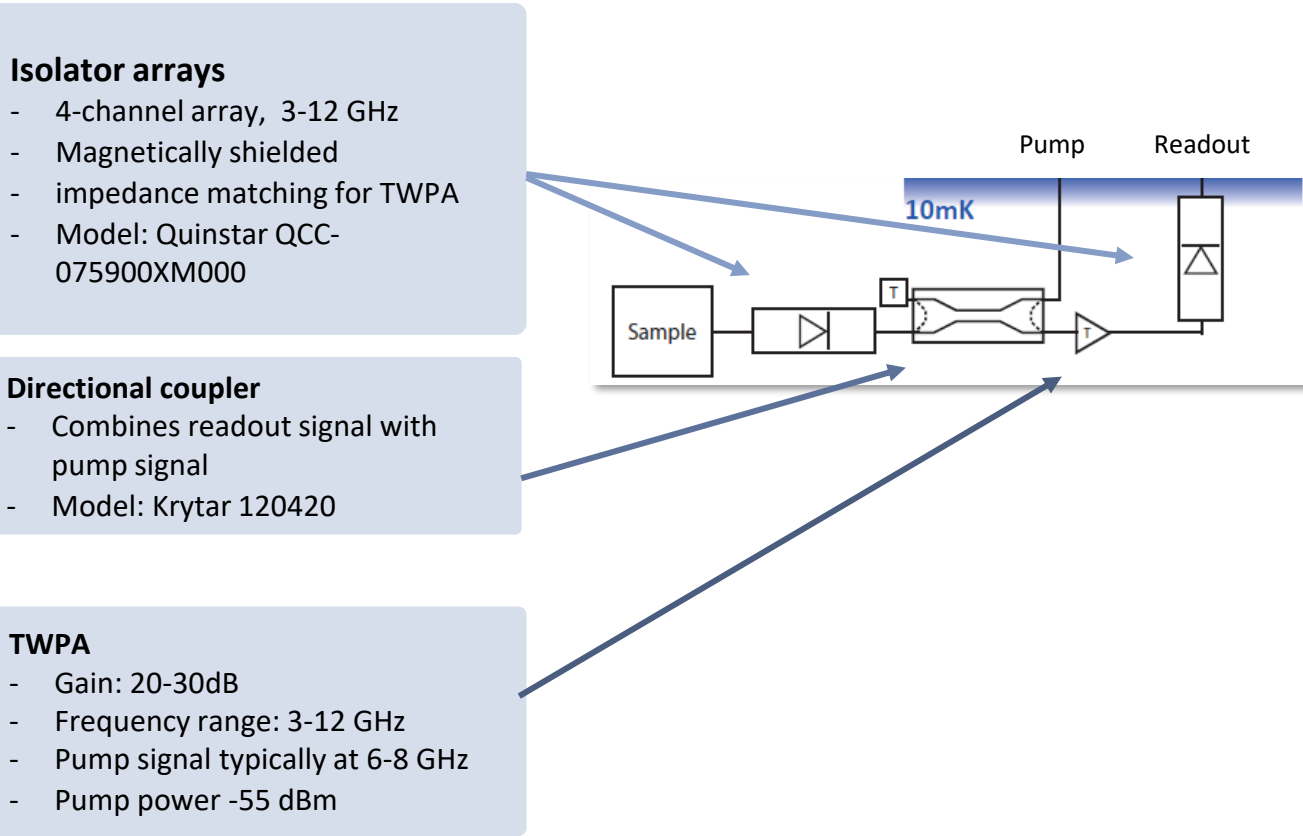
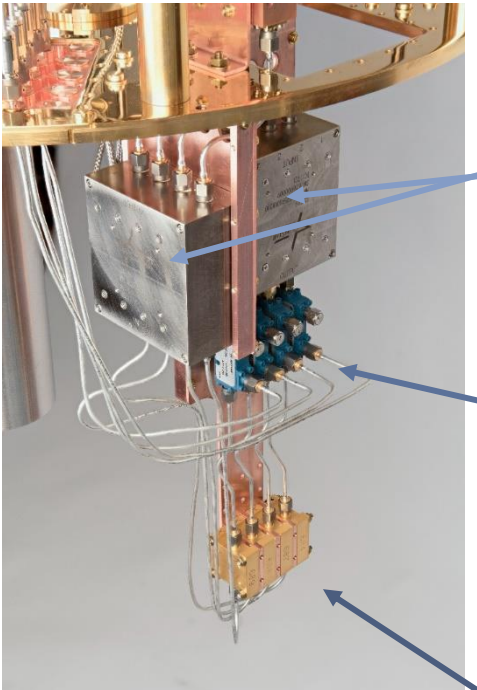


- Mutual inductance between flux line and SQUID typically  $0.5\text{-}1 \Phi_0/\text{mA}$ .
- Fast flux pulses generated by AWG. Static bias by DC source.
- Accurate pulse control at the qubit level requires to characterize the distortion of the pulse when propagating through the flux line and to compensate for it.
- Use qubit as a scope to measure the flux line response function\*.

\*See for example Jerger et al., PRL, 123, 120501 (2019)

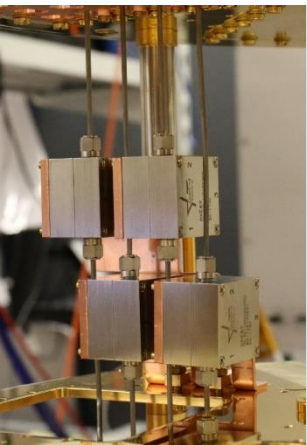


# Output Line Configuration: Active and Passive Components



S. Krinner *et al.*,  
arXiv:1806.07862 (2018)

# Output Line Configuration: Active and Passive Components



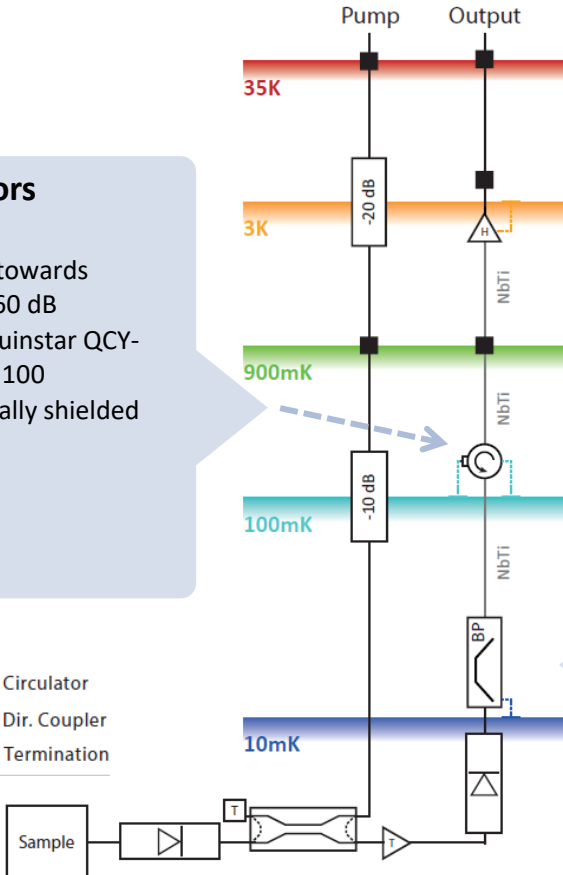
## Circulators

- Isolation towards sample: > 60 dB
- Model: Quinstar QCY-060400CM100
- Magnetically shielded

	Isolator
	TWPA
	HEMT

	Low-pass filter
	Band-pass filter
	Eccosorb filter

	Circulator
	Dir. Coupler
	Termination



## HEMT amplifiers

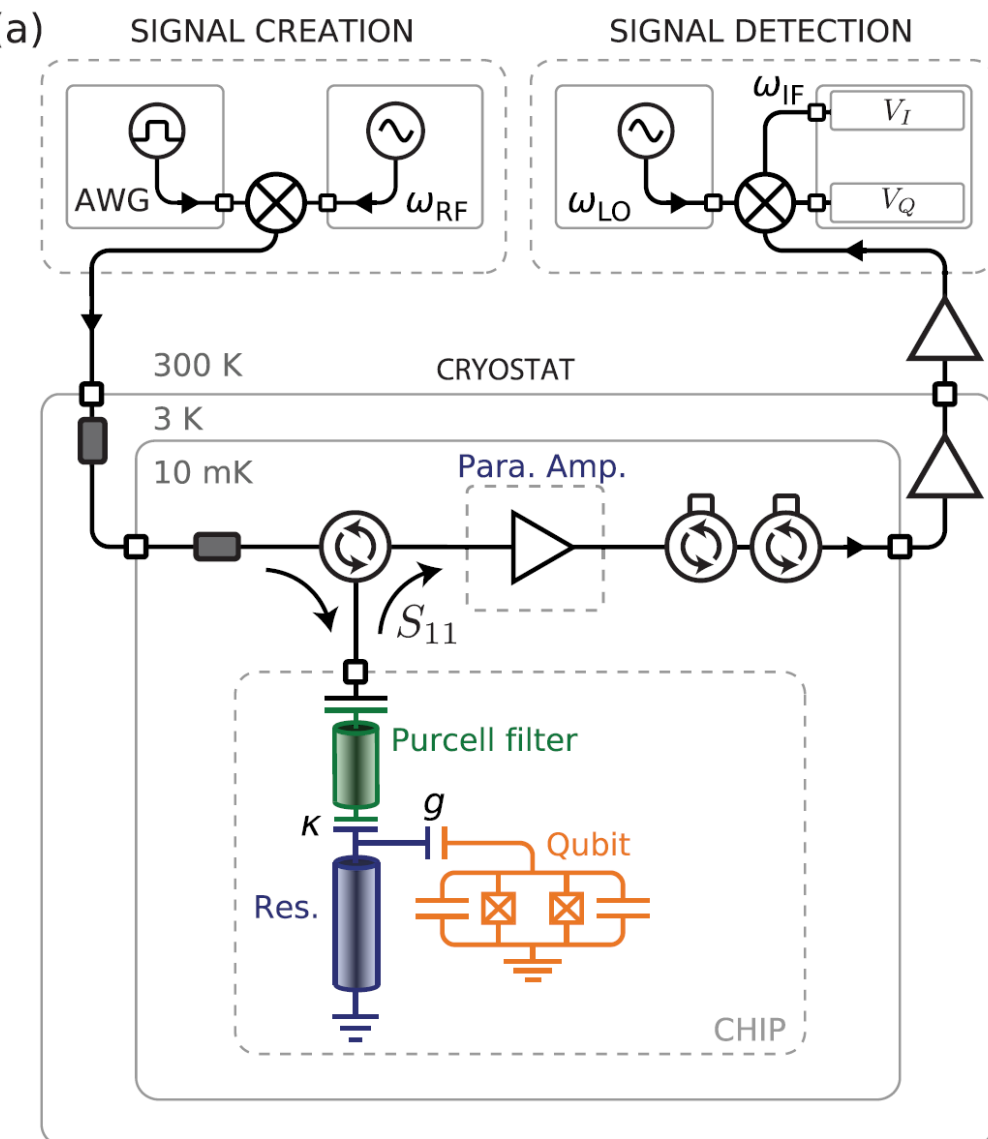
- Gain: ~ 40 dB
- Model: LNF LNC4\_8C



## Bandpass filters

- Bandwidth: 4-8 GHz
- Model: Keenlion KBF-4/8/2S





$$\chi = \chi_{01} + \frac{\chi_{12}}{2} = -\frac{g_{01}^2}{\Delta} \left( \frac{1}{1 + \Delta/\alpha} \right)$$

$$H_{\text{disp}} = (\omega_r + \chi \sigma_z) \left( a^\dagger a + \frac{1}{2} \right) + \frac{\tilde{\omega}_q}{2} \sigma_z$$

$$H_{\text{disp}} = \omega_r \left( a^\dagger a + \frac{1}{2} \right) + \frac{1}{2} \left( \omega_q + \frac{g^2}{\Delta} + \frac{2g^2}{\Delta} a^\dagger a \right) \sigma_z$$

Lamb shift                    ac-Stark shift

$$\bar{n}_c \equiv \Delta^2 / (4g^2)$$

Therefore, the critical photon number sets an upper bound for the power level of the resonator probe signal to maintain (an approximate) QND measurement.

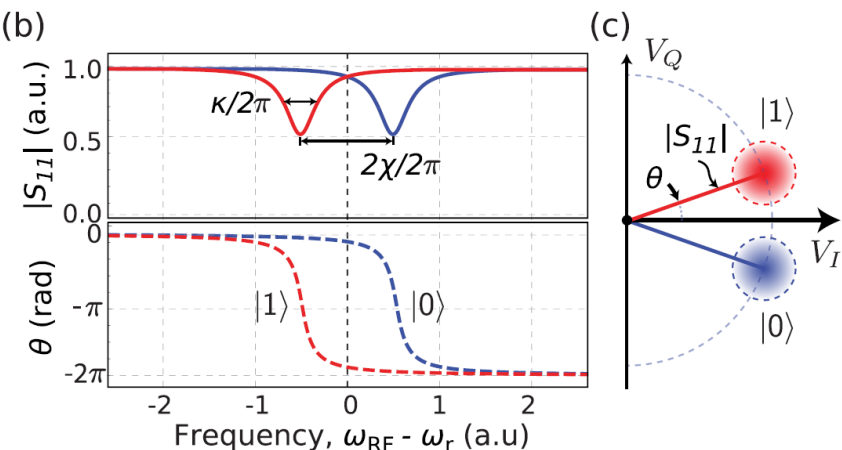


**FIG. 19.** (a) Simplified schematic of a representative experimental setup used for dispersive qubit readout. The resonator probe tone is generated, shaped and timed using an arbitrary waveform generator (AWG), and sent down into the cryostat. The reflected signal  $S_{11}$  is amplified, first in a parametric amplifier and then in a low-noise HEMT amplifier, before it is downconverted using heterodyne mixing and finally sampled in a digitizer. (b) Reflected magnitude  $|S_{11}|$  and phase  $\theta$  response of the resonator with linewidth  $\kappa$ , when the qubit is in its ground state  $|0\rangle$  (blue) and excited state  $|1\rangle$  (red), separated with a frequency  $2\chi/2\pi$ . (c) Corresponding complex plane representation, where each point is composed of the in-plane  $\text{Re}[S_{11}]$  and quadrature  $\text{Im}[S_{11}]$  components. The highest state discrimination is obtained when probing the resonator just in-between the two resonances, [dashed line in (b)], thus maximizing the distance between the states.

# Representation of the Readout Signal

A readout event commences with a short microwave tone directed to the resonator at the resonator probe frequency  $\omega_{\text{RO}}$ . After interacting with the resonator, the reflected (or transmitted) microwave signal has the form

$$s(t) = A_{\text{RO}} \cos(\omega_{\text{RO}} t + \theta_{\text{RO}}), \quad (147)$$

where  $\omega_{\text{RO}}$  is the “carrier frequency” used to probe the resonator.  $A_{\text{RO}}$  and  $\theta_{\text{RO}}$  are, respectively, the qubit-state-dependent amplitude and phase that we want to measure. One can equivalently use a “complex analytic representation” of the signal,

$$\begin{aligned} s(t) &= \text{Re}\{A_{\text{RO}} e^{j(\omega_{\text{RO}} t + \theta_{\text{RO}})}\} \\ &= \text{Re}\{A_{\text{RO}} \cos(\omega_{\text{RO}} t + \theta_{\text{RO}}) + j \sin(\omega_{\text{RO}} t + \theta_{\text{RO}})\} \end{aligned} \quad (148)$$

where  $\text{Re}$  takes the real part of an expression, e.g.,  $\text{Re}[\exp(jx)] = \text{Re}(\cos x + j \sin x) = \cos x$ .

To gain intuition, we can rewrite Eq. (148) in a static “phasor” notation that separates out the time dependence  $\exp(j\omega_{\text{RO}} t)$

$$s(t) = \text{Re} \left\{ \underbrace{A_{\text{RO}} e^{j\theta_{\text{RO}}}}_{\text{phasor}} e^{j\omega_{\text{RO}} t} \right\}, \quad (149)$$

where the phasor  $A_{\text{RO}} \exp(j\theta_{\text{RO}}) \equiv A_{\text{RO}} \angle \theta_{\text{RO}}$  is a shorthand that fully specifies a harmonic signal  $s(t)$  at a known frequency  $\omega_{\text{RO}}$ . To perform qubit readout, we want to measure the “in-phase” component  $I$  and a “quadrature” component  $Q$  of the complex number represented by the phasor

$$A_{\text{RO}} e^{j\theta_{\text{RO}}} = A_{\text{RO}} \cos \theta_{\text{RO}} + j A_{\text{RO}} \sin \theta_{\text{RO}}, \quad (150)$$

$$\equiv I + jQ \quad (151)$$

to determine the amplitude  $A_{\text{RO}}$  and the phase  $\theta_{\text{RO}}$  (Fig. 20).

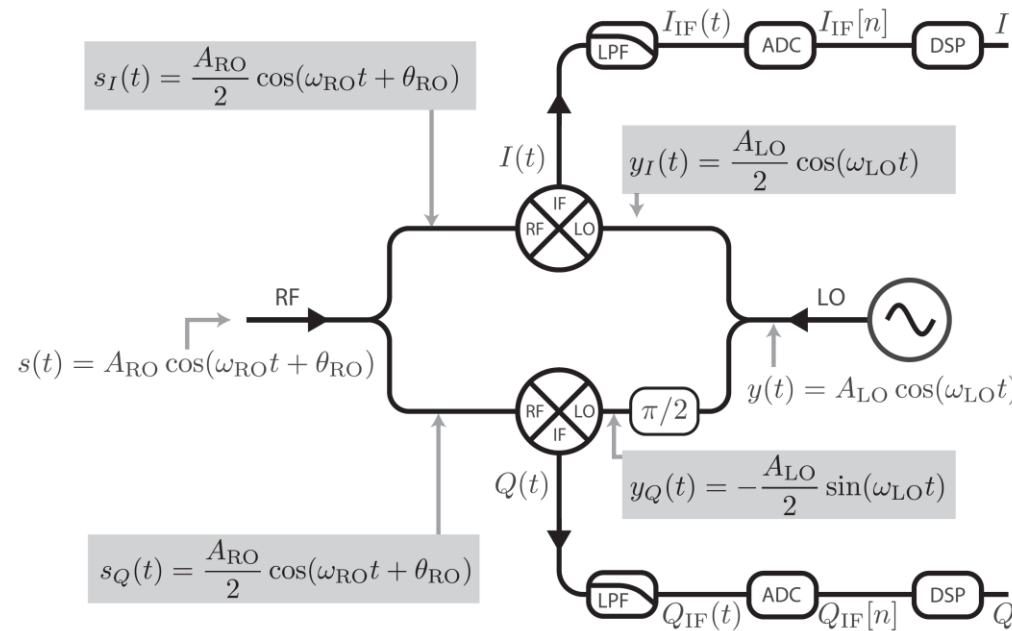


**FIG. 21.** Schematic of an I-Q mixer. A readout pulse at frequency  $\omega_{\text{RO}}$  enters the RF port, where it is equally split into two paths. A local oscillator at frequency  $\omega_{\text{LO}}$  enters the LO port, where it is equally split into two paths, one of which undergoes a  $\pi/2$ -radian phase rotation. To perform analog modulation, the two signals in each path are multiplied at a mixer, yielding the outputs  $I(t)$  and  $Q(t)$ , each having frequencies  $\omega_{\text{RO}} \pm \omega_{\text{LO}}$ .  $I(t)$  and  $Q(t)$  are then low-pass-filtered (time averaged) to yield  $I_{\text{IF}}(t)$  and  $Q_{\text{IF}}(t)$  at the intermediate frequency  $\omega_{\text{IF}} = |\omega_{\text{RO}} - \omega_{\text{LO}}|$ , and subsequently digitized using an analog-to-digital (ADC) converter. If  $\omega_{\text{IF}} \neq 0$ , then digital signals  $I_{\text{IF}}[n]$  and  $Q_{\text{IF}}[n]$  are further digitally demodulated using digital signal processing (DSP) techniques to extract the amplitude and phase of the readout signal.

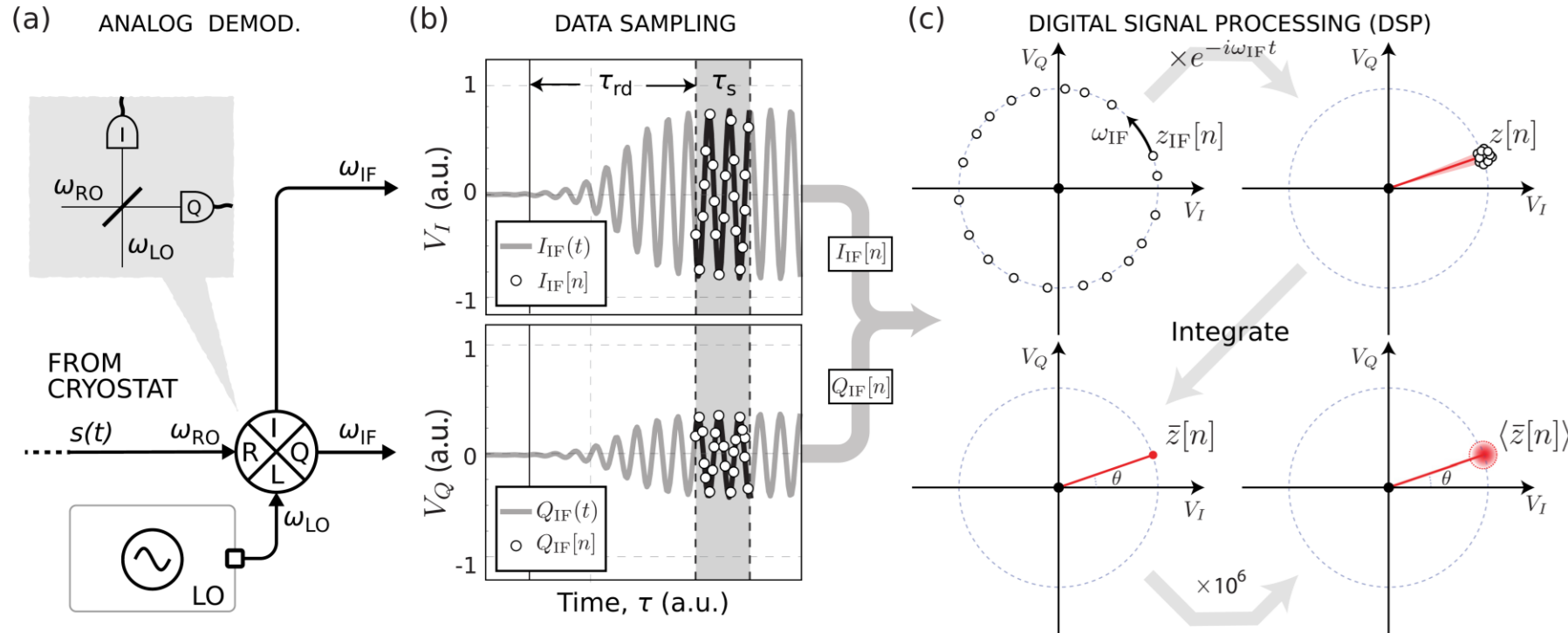


**FIG. 22.** Schematic of the heterodyne detection technique. (a) The signal with frequency  $\omega_{\text{RF}}$  from the cryostat is mixed with a carrier tone with frequency  $\omega_{\text{LO}}$ , yielding two quadratures at a down-converted intermediate frequency  $\omega_{\text{IF}} = |\omega_{\text{RO}} - \omega_{\text{LO}}|$ , and  $90^\circ$  out-of-phase with each other. (b) The two signals are passed into two different analog-to-digital converter (ADC) channels. To avoid sampling the resonator transient, some readout delay ( $\tau_{\text{rd}}$ ) corresponding to the resonator linewidth may be added, and the two signals are sampled for a time  $\tau_s$ . In this case, the white dots represent the sampled points. (c) The sampled traces are postprocessed and after some algebra, the sampled data points are averaged into a single point in the  $(I, Q)$ -plane. To extract statistics of the readout performance, i.e., single-shot readout fidelity, a large number of  $(I, Q)$ -records are acquired, yielding a 2D-histogram, with a Gaussian distributed spread given by the noise acting on the signal.